

A Simplified Modulated Model Predictive Control for a Grid-Tied Three-Level T-Type Inverter

Xu, Junzhong; Soeiro, Thiago Batista; Gao, Fei; Tang, Houjun; Bauer, Pavol

DOI

[10.1109/ISIE45063.2020.9152376](https://doi.org/10.1109/ISIE45063.2020.9152376)

Publication date

2020

Document Version

Final published version

Published in

2020 IEEE 29th International Symposium on Industrial Electronics (ISIE)

Citation (APA)

Xu, J., Soeiro, T. B., Gao, F., Tang, H., & Bauer, P. (2020). A Simplified Modulated Model Predictive Control for a Grid-Tied Three-Level T-Type Inverter. In *2020 IEEE 29th International Symposium on Industrial Electronics (ISIE): Proceedings* (pp. 618-623). Article 9152376 IEEE.
<https://doi.org/10.1109/ISIE45063.2020.9152376>

Important note

To cite this publication, please use the final published version (if applicable).
Please check the document version above.

Copyright

Other than for strictly personal use, it is not permitted to download, forward or distribute the text or part of it, without the consent of the author(s) and/or copyright holder(s), unless the work is under an open content license such as Creative Commons.

Takedown policy

Please contact us and provide details if you believe this document breaches copyrights.
We will remove access to the work immediately and investigate your claim.

A Simplified Modulated Model Predictive Control for a Grid-Tied Three-Level T-Type Inverter

Junzhong Xu¹, Thiago Batista Soeiro², Fei Gao¹, Houjun Tang¹, Pavol Bauer²

1: Department of Electrical Engineering, Shanghai Jiao Tong University, Shanghai, China

2: DCE&S group, Delft University of Technology, Delft, The Netherlands

Junzhongxu@sjtu.edu.cn, T.BatistaSoeiro@tudelft.nl, Fei.gao@sjtu.edu.cn, Hjtang@sjtu.edu.cn, P.Bauer@tudelft.nl

Abstract—The implementation of finite-control-set model predictive control (FCS-MPC) in grid-tied inverters can make the system to suffer from poor harmonics performance, which may complicate the AC filter design for compliance with strict harmonic standards. To overcome this shortcoming, a simplified modulated model predictive control strategy is proposed in this paper. This control strategy not only improves current waveform total harmonic distortion (THD) without introducing additional weight factor in the cost function but can also shorten running/computational time without compromising the performance of fast current dynamic response. Herein, the detailed implementation of this control strategy is given, while considering its application to the current feedback control loop of a three-phase three-level T-type inverter modulated at constant switching frequency. Finally, PLECS circuit simulations are used to verify the feasibility and effectiveness of the proposed control strategy and to benchmark its performance to the classical FCS-MPC strategy and the application of a PI-controller.

Index Terms—Finite-control-set model predictive control (FCS-MPC), modulated model predictive control (MMPC), three-level T-type NPC inverter

I. INTRODUCTION

THREE-LEVEL neutral-point-clamped (3L-NPC) voltage source inverters are widely used in motor drives and renewable energy systems due to their lower harmonics, smaller filter size, increased efficiency, and higher power density, in comparison to the traditional two-level inverters [1]–[3]. The research [4] has shown that in low voltage applications, the utilization of a 3L-T-type inverter as an alternative for the conventional diode-clamped 3L-NPC inverter can be advantageous for moderated switching frequencies, e.g., < 12kHz. The main advantages of the T-type structure are: it requires two fewer power diodes; with similar design ratings to the diode-clamped 3L-NPC inverter, it can provide lower conduction losses (but higher switching losses) [5]. With the increasing utilization of the T-type circuit technology in solar and motor drive applications, the interest to the control scheme of this inverter has gained momentum in both industry and academia [6]–[15].

Among various control methods, the model predictive control (MPC) has become a popular topic of research, particularly because of the recent development of high performance microprocessors [6]. The MPC has many exciting features, among all it can lead to fast dynamic responses, and it is an intuitive concept of relatively easy implementation. In particular, finite-control-set model predictive control (FCS-

MPC) has been successfully applied to a 3L-NPC inverter [7]. Without any modulator, the conventional FCS-MPC uses only a finite number of available switching states to operate the converter to predict all the feasible future behaviors and consequent performances to select an optimal switching state. This runs as an optimization routine minimizing a predefined cost function to achieve the prioritized control objectives.

A fast-predictive control method (with a faster run-time implementation) has been presented in [8]. This uses the analytical model equations of the system just once in each control cycle to predict the optimal vector. Interestingly, the number of voltage vectors involved in the analytical model can also be reduced from 27 to 3, and by consequence, the computational efficiency will be greatly improved while using the fast finite-switching-state MPC (FSS-MPC) algorithm proposed in [9].

A simplified model predictive control (SMPC) strategy is studied in [10] for a 3L-T-type inverter, which is aimed to reduce the computation burden while achieving robust and fast current feedback control, the necessary capacitor voltage balance and improvements in common-mode voltage (CMV) generation. With the equivalent transformation and specialized sector distribution method in [11], the computation time of the FCS-MPC can be effectively reduced while the system performance is not compromised. However, since FCS-MPC utilizes only one switching state for the whole sampling interval, the controller will generate the output waveform with a variable switching frequency, which can negatively affect the generated voltage/current waveform harmonic spectrum, making the design of harmonic and EMC filters complicated.

Several advanced strategies have been proposed to improve the output current quality of a 3L-NPC inverter. In [12] and [13], as an extension of the modulated model predictive control (MMPC) in a two-level rectifier [16], a current predictive control with fixed switching frequency was proposed. Based on [12] and [13], a finite-set MPC strategy with fixed switching frequency is developed in the grid-tied application [14], which utilizes the redundant vectors to balance the partial DC capacitor voltages. Based on the discrete space vector modulation, an improved FCS-MPC able to reduce current ripples and to balance the neutral-point voltage for the 3L-NPC inverter is studied in [15]. However, an extra computation time for the FCS-MPC is necessary to realize a fixed switching sequence and space vector modulation.

This paper proposes a simplified MMPC for a grid-tied

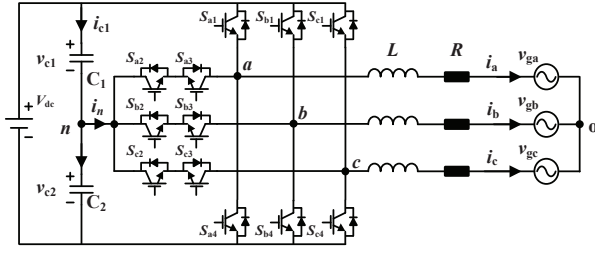


Fig. 1. Three-phase T-type inverter.

TABLE I
SWITCHING STATES ($x = a, b, c$)

S_x	S_{x1}	S_{x2}	S_{x3}	S_{x4}	v_{xn}
1	1	1	0	0	$V_{dc}/2$
0	0	1	1	0	0
-1	0	0	1	1	$-V_{dc}/2$

three-phase 3L-T-type inverter able to reduce the computational time without affecting the control performance. Different from the traditional MMPC studied in [12], the candidate switching vectors are preselected based on the sector distribution. This simplifies the application of an MMPC in the T-type circuit. Furthermore, the current total harmonic distortion (THD) will be reduced at fixed switching frequency without introducing additional weight factor in the cost function. The paper is divided as follows. In section II the analytical model of the three-phase 3L-T-type inverter is derived. In Section III and IV, the detailed implementation of the classic FCS-MPC and proposed simplified MMPC is given, respectively. Finally, in Section V a PLECS based simulation of a 3L-T-type inverter running the simplified MMPC is used to verify the effectiveness of the proposed method.

II. MODELING OF THE THREE-PHASE 3L-T-TYPE INVERTER

A three-phase 3L-T-type inverter is shown in Fig. 1. The basic converter is composed of 12 active switches, two series-connected DC capacitors C_1 and C_2 , and a L filter at the AC or grid side. Although the switches S_{x1} and S_{x4} have to block the total DC voltage V_{dc} , they can be operated to switch only the partial DC capacitor voltages or ideally half of V_{dc} . The switches S_{x2} and S_{x3} have to block the partial DC capacitor voltages. Note that in Fig. 1, v_{ga} , v_{gb} and v_{gc} represent the grid phase voltages; while i_a , i_b and i_c represent the output currents of the inverter; L refers to the filter inductance; and R is the total equivalent resistance between the inverter and the grid, mostly defined by the parasitic winding resistances of L . The switching states and the corresponding converter terminal voltages are shown in Table I. Each phase of the T-type 3L-NPC inverter can generate the following three output states depending upon different switch combinations: "1", "0" and "-1" states. It can be seen that: (a) in the "1" state S_{x1} and S_{x2} are turned ON while S_{x3} and S_{x4} are turned OFF, and the phase output voltage from the AC terminal x with reference to

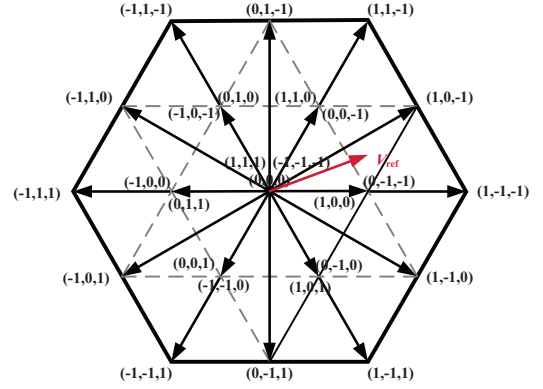


Fig. 2. Space vector diagram for a three-level T-type inverter.

the terminal n (or the mid-point of the DC-link capacitors) is $v_{xn} = V_{dc}/2$; (b) in the "0" state S_{x2} and S_{x3} are turned ON while S_{x1} and S_{x4} are switched OFF, and $v_{xn} = 0$; (c) in the "-1" state S_{x4} and S_{x3} are turned ON while S_{x1} and S_{x2} are switched OFF, and $v_{xn} = -V_{dc}/2$. A total of 27 (3^3) switching combinations are available for the converter operation, which are represented in Fig. 2.

According to the current i_a , i_b and i_c flow directions in Fig. 1, the output current dynamics in α - β coordinate can be expressed as:

$$\begin{cases} L \frac{di_\alpha}{dt} = v_{\alpha n} - v_{g\alpha} - Ri_\alpha \\ L \frac{di_\beta}{dt} = v_{\beta n} - v_{g\beta} - Ri_\beta \end{cases} \quad (1)$$

The currents through the capacitor can be expressed as:

$$\begin{cases} C_1 \frac{dv_{c1}}{dt} = i_{c1} \\ C_2 \frac{dv_{c2}}{dt} = i_{c2} \end{cases} \quad (2)$$

For the digital control implementation of the circuit in a microcontroller, the model of the inverter must be defined as a discrete-time model [7]. The derivative of the AC line currents and the capacitor voltages in the continuous-time model can be approximated based on the forward Euler approximation with the analog-to-digital conversion sampling period T_s as:

$$\frac{di_{\alpha\beta}}{dt} \approx \frac{i_{\alpha\beta}[k+1] - i_{\alpha\beta}[k]}{T_s} \quad (3)$$

$$\frac{du_c}{dt} \approx \frac{u_c[k+1] - u_c[k]}{T_s} \quad (4)$$

Thereafter, (1) and (2) can be re-written in the discrete form:

$$\begin{cases} i_\alpha[k+1] = \frac{L-RT_s}{L} i_\alpha[k] + \frac{T_s}{L} (v_{\alpha n}[k] - v_{g\alpha}[k]) \\ i_\beta[k+1] = \frac{L-RT_s}{L} i_\beta[k] + \frac{T_s}{L} (v_{\beta n}[k] - v_{g\beta}[k]) \end{cases} \quad (5)$$

$$\begin{cases} v_{c1}[k+1] = v_{c1}[k] + \frac{T_s}{C_1} i_{c1}[k+1] \\ v_{c2}[k+1] = v_{c2}[k] + \frac{T_s}{C_2} i_{c2}[k+1] \end{cases} \quad (6)$$

III. THE CLASSIC FCS-MPC FOR THE 3L-T-TYPE INVERTER

A. Control Strategy

The feedback current control of the inverter based on the FCS-MPC technique is known for utilizing only a finite

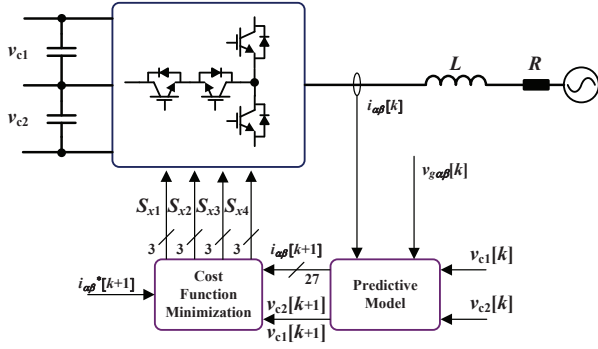


Fig. 3. Block diagram of conventional FCS-MPC [6].

number of possible switching states that can be generated by the power converter during the optimization routines. This method can predict well the behavior of the modeled system variables and specific performance indexes for each analyzed switching state [6]. Herein, the reasoning is that each current $i_{\alpha,\beta}$ and $v_{c1,c2}$ prediction is evaluated with respect to its references $i_{\alpha,\beta}^*$ and $v_{c1,c2}^*$ in a cost function, and the switching state that generates the minimum deviation (or error) value is selected to be applied in the next sampling time.

The block diagram of this control strategy for the 3L-T-type inverter is shown in Fig. 3. The main control objectives are the regulation of the AC line currents and the balance of the DC-link partial voltages. The FCS-MPC method uses the discrete-models of the system developed in Section II, i.e., the AC currents and DC-link capacitor voltages analytical models, and all the 27 possible switching states to predict the future behavior of the controlled variables.

B. Cost Function Design

The defined cost function has two objectives: (a) to minimize the error between the predicted load currents $i_{\alpha\beta}[k+1]$ and their references $i_{\alpha\beta}^*[k+1]$, and (b) to balance the DC-link capacitor voltages. These control objectives with the weighting factor λ_{dc} are represented as follows:

$$G = |i_{\alpha}^*[k+1] - i_{\alpha}[k+1]| + |i_{\beta}^*[k+1] - i_{\beta}[k+1]| + \lambda_{dc}|v_{c1}[k+1] - v_{c2}[k+1]| \quad (7)$$

IV. PROPOSED MODULATED MODEL PREDICTIVE CONTROLLER FOR THE 3L-T-TYPE INVERTER

The proposed simplified MMPC includes a suitable modulation scheme in the cost function minimization. Fig. 4 shows the block diagram of the MMPC. Similar to the FCS-MPC strategy, it uses the prediction of the AC line currents and capacitor voltages based on (5) and (6), respectively. At every sampling time and depending on which one of the six current sectors the system operates, the MMPC evaluates the parametric predictions of the two active and two redundant small vectors, and finally solves the cost function separately for each prediction.

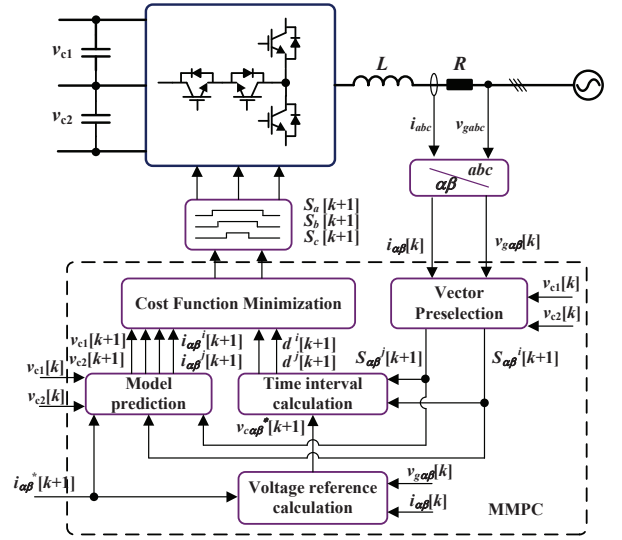
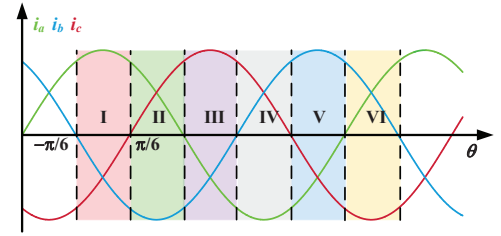
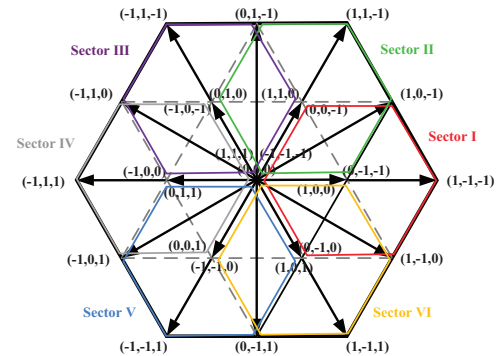


Fig. 4. Block diagram of MMPC for T-type 3L-NPC inverter.



(a)



(b)

Fig. 5. Sector allocation and candidate voltage vectors for the T-type 3L-NPC inverter. (a) Sector allocation, (b) candidate voltage vectors.

A. Vector Pre-selection

The converter voltage vectors are divided into six sectors according to the input three-phase current polarity as shown in Fig. 5(a), and the candidate voltage states to be applied in each sector are shown in Fig. 5(b). Based on the conventional space-vector modulation, if the target vector is located in one triangle, then its vertex vectors are used to realize the target vector. One of the three nearest vectors forming the triangle in question is always the redundant vector pointing to the center of the active hexagon. To reduce the number of the processed switching vectors, the candidate switching states (S_a, S_b, S_c)

TABLE II
FEASIBLE SWITCHING VECTORS IN SECTOR I

S	(S_a^0, S_b^0, S_c^0)	(S_a, S_b, S_c)
0	(0, 0, 0)	(0, -1, -1)
1	(0, 0, 1)	(0, -1, 0)
2	(0, 1, 0)	(0, 0, -1)
3	(0, 1, 1)	(0, 0, 0)
4	(1, 0, 0)	(1, -1, -1)
5	(1, 0, 1)	(1, -1, 0)
6	(1, 1, 0)	(1, 0, -1)
7	(1, 1, 1)	(1, 0, 0)

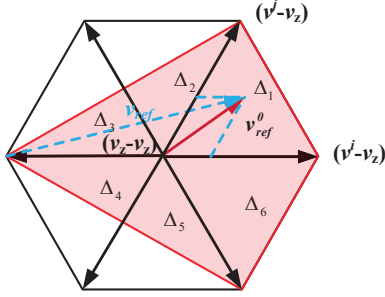


Fig. 6. Synthesis of equivalent reference voltage vector in two-level equivalent space vector diagram.

for six active vectors and two redundant vectors in each sector can be obtained by:

$$S_i = S_i^0 + 0.5[\text{sign}(i_x) - 1], \quad x \in \{a, b, c\} \quad (8)$$

where (S_a^0, S_b^0, S_c^0) is the basic switching state. $\text{sign}(i_x) = 1$ when $i_x \geq 0$, otherwise $\text{sign}(i_x) = -1$. Taking sector I as an example, the eight candidate switching states are summarized in Table II. The candidate switching states in another sector can be pre-selected in the same way.

Once the sector is determined, the origin of a reference voltage vector can be changed to the center voltage vector of the selected hexagon v_z . Since v_z has two switching state realizations, it can be split into its two realizations, namely v_0^0 and v_7^0 . This is done by subtracting the center vector of the selected hexagon from the original reference vector, as shown in Fig. 6. In Fig. 6 v_{ref}^0 is the original reference voltage vector and v_{ref}^θ is the corrected reference voltage vector seen from the location of the center vector v_z .

In order to implement a SVM algorithm in the MMPC, the space vector diagram of each sector shown in Fig. 6 is divided into 6 triangles (denoted as Δ_n with $n \in \{1, \dots, 6\}$), where each triangle Δ_n is composed of two equivalent active vectors v_i^0 and v_j^0 and the two equivalent zero vectors v_0^0 and v_7^0 . For the implementation of the SVM, a symmetrical pulse pattern is adopted in this work. An example of this sequence for the Δ_1 of sector I is defined in Fig. 7.

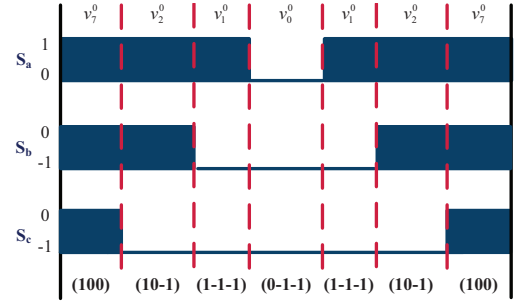


Fig. 7. MMPC switching pattern in the Δ_1 of Sector I.

B. Converter Voltage Reference Calculation

Based on (5), the current predictions can be rewritten as:

$$\begin{cases} i_\alpha[k+1] = i_\alpha^z[k+1] - \frac{T_s}{L} v_\alpha^0[k] \\ i_\beta[k+1] = i_\beta^z[k+1] - \frac{T_s}{L} v_\beta^0[k] \end{cases} \quad (9)$$

where (i_α^z, i_β^z) represents the evolution of the system, when the redundant vector v_z is applied. (v_α^0, v_β^0) is the corrected reference voltage vector v_{ref}^0 , which is defined by:

$$\begin{cases} v_\alpha^0 = d_i(v_{i\alpha}^0 - v_{z\alpha}) + d_j(v_{j\alpha}^0 - v_{z\alpha}) \\ v_\beta^0 = d_i(v_{i\beta}^0 - v_{z\beta}) + d_j(v_{j\beta}^0 - v_{z\beta}) \end{cases} \quad (10)$$

where $(v_{i\alpha}^0, v_{i\beta}^0)$ and $(v_{j\alpha}^0, v_{j\beta}^0)$ are two candidate voltage vectors selected by the MMPC algorithm, and d_i and d_j are their associated duty cycles.

Assuming that the predicted currents match the current references, the voltage references (v_α^*, v_β^*) can be defined as:

$$\begin{cases} v_\alpha^*[k+1] = \frac{L}{T_s}(i_\alpha^z[k+1] - i_\alpha^*[k+1]) \\ v_\beta^*[k+1] = \frac{L}{T_s}(i_\beta^z[k+1] - i_\beta^*[k+1]) \end{cases} \quad (11)$$

C. Current Predictions

According to Table II, the current predictions are calculated for each one of the candidate adjacent vectors (v_i^0, v_j^0) considering both vectors applied in one sampling interval:

$$\begin{cases} i_\alpha^i[k+1] = i_\alpha^z[k+1] - \frac{T_s}{L} d_i(v_\alpha^i[k+1] - v_{z\alpha}[k]) \\ i_\beta^i[k+1] = i_\beta^z[k+1] - \frac{T_s}{L} d_i(v_\beta^i[k+1] - v_{z\beta}[k]) \end{cases} \quad (12)$$

$$\begin{cases} i_\alpha^j[k+1] = i_\alpha^z[k+1] - \frac{T_s}{L} d_j(v_\alpha^j[k+1] - v_{z\alpha}[k]) \\ i_\beta^j[k+1] = i_\beta^z[k+1] - \frac{T_s}{L} d_j(v_\beta^j[k+1] - v_{z\beta}[k]) \end{cases} \quad (13)$$

where

$$(i, j) = (1, 2), (2, 3), (3, 4), (4, 5), (5, 6), (6, 1). \quad (14)$$

D. Duty Cycle Calculations

The duty cycles are calculated based on the voltage reference derived from (11) for each one of the two active vectors:

$$\begin{cases} v_\alpha^* = d_i(v_{i\alpha}^0 - v_{z\alpha}) + d_j(v_{j\alpha}^0 - v_{z\alpha}) + v_{z\alpha} \\ v_\beta^* = d_i(v_{i\beta}^0 - v_{z\beta}) + d_j(v_{j\beta}^0 - v_{z\beta}) + v_{z\beta} \end{cases} \quad (15)$$

TABLE III
SIMULATION PARAMETERS

Variables	Parameters	Value
V_{dc}	DC voltage	700 V
V_g	Grid RMS voltage	220 V
C_1, C_2	Partial DC capacitance	470 μ F
f_g	Grid frequency	50 Hz
R	Parasitic resistor	0.1 Ω
L	Inductive filter	600 μ H

Solving the above equation, the duty cycles for each pair of vectors can be defined by:

$$\begin{cases} d_i = \frac{(v_\beta^* - v_z\beta)(v_{j\alpha}^0 - v_z\alpha) - (v_\alpha^* - v_z\alpha)(v_{j\beta}^0 - v_z\beta)}{(v_{j\alpha}^0 - v_z\alpha)(v_{i\beta}^0 - v_z\beta) - (v_{i\alpha}^0 - v_z\alpha)(v_{j\beta}^0 - v_z\beta)} \\ d_j = \frac{(v_\beta^* - v_z\beta)(v_{i\alpha}^0 - v_z\alpha) - (v_\alpha^* - v_z\alpha)(v_{i\beta}^0 - v_z\beta)}{(v_{i\alpha}^0 - v_z\alpha)(v_{j\beta}^0 - v_z\beta) - (v_{j\alpha}^0 - v_z\alpha)(v_{i\beta}^0 - v_z\beta)} \end{cases} \quad (16)$$

Thereafter, the duty cycle of the selected center voltage vector d_z can be calculated:

$$d_z = 1 - d_i - d_j. \quad (17)$$

E. Cost Function Minimization

A single-objective predictive controller regulates the grid currents using the following cost function:

$$\begin{aligned} G &= G_i + G_j \\ G_i &= d_i \sqrt{(i_\alpha^i - i_\alpha^*)^2 + (i_\beta^i - i_\beta^*)^2} \\ G_j &= d_j \sqrt{(i_\alpha^j - i_\alpha^*)^2 + (i_\beta^j - i_\beta^*)^2} \end{aligned} \quad (18)$$

The pair of vectors with the minimum value of G is selected to be applied for the associated duty cycles d_i and d_j .

F. Capacitor Voltage Balancing

Negative and positive small vectors v_0^0 and v_7^0 have an opposite effect in the current injected at the neutral-point terminal n . The ratio between the negative and positive duty cycles are redistributed as a function of the following imbalance index:

$$\Delta v_b = \frac{v_{c1} - v_{c2}}{v_{c1} + v_{c2}} \quad (19)$$

which is bounded between (-1, 1). Thus, duty cycles of v_0^0 and v_7^0 are calculated as follows:

$$d_z^- = \frac{1 - \Delta v_b}{2} d_z \quad (20)$$

$$d_z^+ = \frac{1 + \Delta v_b}{2} d_z \quad (21)$$

V. SIMULATION RESULTS

To validate the effectiveness of the proposal MMPC applied to the 3L-T-type inverter, PLECS based simulation results are presented during both steady-state and dynamic-state test conditions. These results are compared with the ones obtained with the same inverter employing the classical FCS-MPC strategy or the traditional PI-controller. The simulation parameters are shown in Table III. To have a reasonable

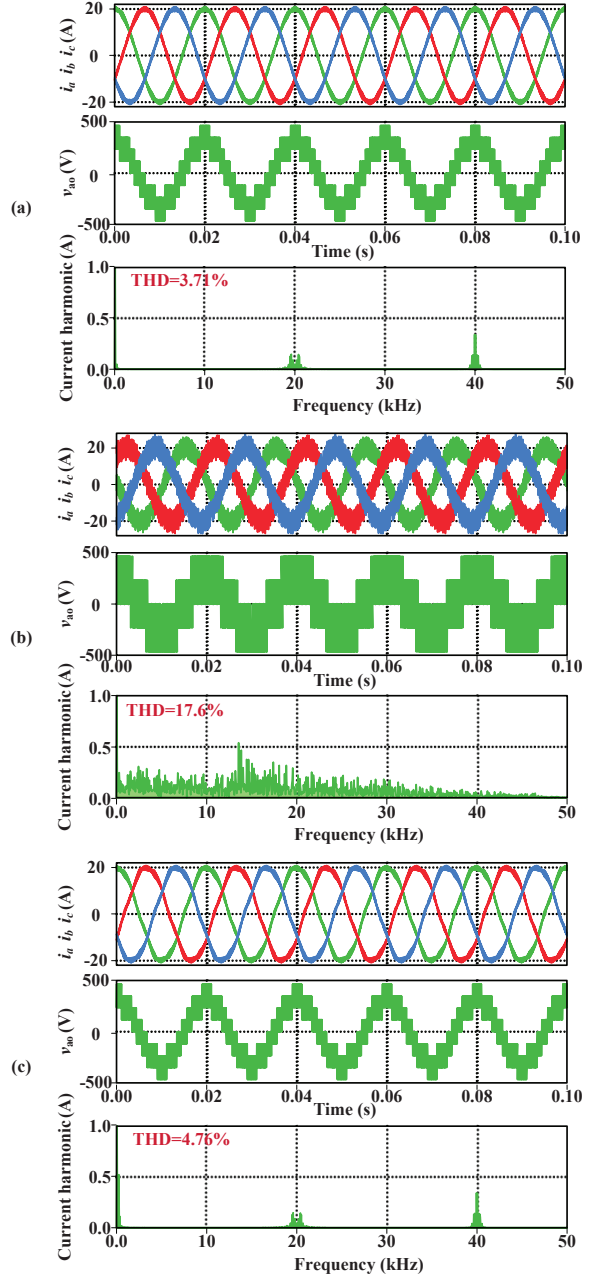


Fig. 8. Steady-state simulation waveforms showing the grid currents, the output terminal voltage v_{a0} , and phase current harmonics for implementation of (a) the proposed MMPC, (b) the conventional MPC, (c) the PI-controller.

comparison between the proposed and the classical predictive control methods, a shorter sampling time T_s is considered for the traditional predictive controller, where $T_s = 1/60000$ s, while a $T_s = 1/20000$ s is defined for the proposed MMPC and PI-controller. The switching frequency of the MMPC and PI-controller is the same as the sampling frequency, $f_{sw} = 20$ kHz.

A. Results During Steady State Operation

The steady-state waveforms for the three-phase grid currents, the inverter generated terminal voltage a with reference

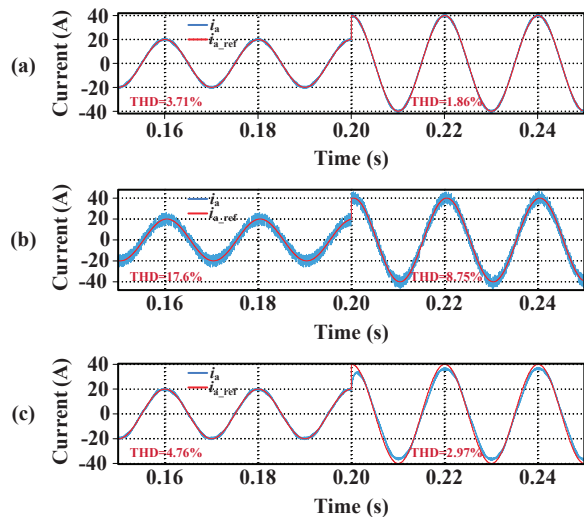


Fig. 9. Dynamic-state simulation waveform for grid current i_a and its reference i_{a_ref} (a) proposed MMPC, (b) conventional MPC, (c) PI-controller.

to the grid neutral terminal o , and the current harmonic spectrum obtained with the proposed MMPC, the conventional FCS-MPC, and the PI-controller are shown in Fig. 8, where the magnitude of the reference current is set as 20 A. From the current spectrum analysis, one can observe that the proposed MMPC produces a current with a constant switching frequency of 20 kHz, while the FCS-MPC control has a variable switching frequency, which is mostly lower than 20 kHz. Finally, the implemented FCS-MPC method presents a higher value of THD compared to the proposed MMPC, and the AC line current ripple for the MMPC is slightly lower than that of the PI-controller.

B. Results During Dynamic State Operation

To demonstrate the performance of the proposed control strategy in terms of dynamic response, transient analysis is carried out with all control methods. Fig. 9 shows the results for grid current i_a and its reference i_{a_ref} , where a step-change in the AC line current reference i_{a_ref} from 20 A to 40 A is applied at the instant of $t = 0.2$ s. In every case, it is observed that the grid current i_a can effectively track i_{a_ref} . The results also attest that the proposed MMPC can have an excellent dynamic response as the conventional MPC. As expected both predictive controls tracking performance are much faster than the one achieved by the PI-controller.

VI. CONCLUSION

This paper has proposed a simplified modulated model predictive control (MMPC) with fixed switching frequency for a three-phase 3L-T-type inverter. This control method implements a MMPC with sector pre-selection, where the number of finite switching states is reduced, and the running time (or computational effort) required by the cost function calculations of the optimization loop is reduced. Compared with the classic FCS-MPC, it solves the problem of the converter generation of a wide spectrum of voltage/current

harmonic content without affecting the control performance in terms of fast dynamic response. PLECS based simulations have verified the effectiveness and superiority of the proposed MMPC method.

ACKNOWLEDGMENT

This work is supported in part by the scholarship from China Scholarship Council (CSC) under the Grant: CSC NO. 201906230170.

REFERENCES

- [1] J. Rodriguez, S. Bernet, P. K. Steimer, and I. E. Lizama, "A survey on neutral-point-clamped inverters," *IEEE Trans. Ind. Electron.*, vol. 57, no. 7, pp. 2219–2230, July 2010.
- [2] S. Kouro, M. Malinowski, K. Gopakumar, J. Pou, L. G. Franquelo, B. Wu, J. Rodriguez, M. A. Pérez, and J. I. Leon, "Recent advances and industrial applications of multilevel converters," *IEEE Trans. Ind. Electron.*, vol. 57, no. 8, pp. 2553–2580, Aug 2010.
- [3] J. I. Leon, S. Kouro, L. G. Franquelo, J. Rodriguez, and B. Wu, "The essential role and the continuous evolution of modulation techniques for voltage-source inverters in the past, present, and future power electronics," *IEEE Trans. Ind. Electron.*, vol. 63, no. 5, pp. 2688–2701, May 2016.
- [4] M. Schweizer and J. W. Kolar, "Design and implementation of a highly efficient three-level T-Type converter for low-voltage applications," *IEEE Trans. Power Electron.*, vol. 28, no. 2, pp. 899–907, Feb 2013.
- [5] U. Choi, F. Blaabjerg, and K. Lee, "Reliability improvement of a T-Type three-level inverter with fault-tolerant control strategy," *IEEE Trans. Power Electron.*, vol. 30, no. 5, pp. 2660–2673, May 2015.
- [6] S. Kouro, P. Cortes, R. Vargas, U. Ammann, and J. Rodriguez, "Model predictive control—a simple and powerful method to control power converters," *IEEE Trans. Ind. Electron.*, vol. 56, no. 6, pp. 1826–1838, June 2009.
- [7] R. Vargas, P. Cortes, U. Ammann, J. Rodriguez, and J. Pontt, "Predictive control of a three-phase neutral-point-clamped inverter," *IEEE Trans. Ind. Electron.*, vol. 54, no. 5, pp. 2697–2705, Oct 2007.
- [8] J. D. Barros, J. F. A. Silva, and E. G. A. Jesus, "Fast-predictive optimal control of NPC multilevel converters," *IEEE Trans. Ind. Electron.*, vol. 60, no. 2, pp. 619–627, Feb 2013.
- [9] Y. Yang, H. Wen, M. Fan, M. Xie, and R. Chen, "Fast finite-switching-state model predictive control method without weighting factors for T-Type three-level three-phase inverters," *IEEE Trans. Ind. Informat.*, vol. 15, no. 3, pp. 1298–1310, March 2019.
- [10] E. Aswani Kumar, R. Srinivasa Rao, and K. Chandra Sekhar, "Simplified model predictive control of a three-phase T-type NPC inverter," *IET Power Electron.*, vol. 12, no. 8, pp. 1917–1930, 2019.
- [11] C. Xia, T. Liu, T. Shi, and Z. Song, "A simplified finite-control-set model-predictive control for power converters," *IEEE Trans. Ind. Informat.*, vol. 10, no. 2, pp. 991–1002, May 2014.
- [12] M. Rivera, M. Perez, V. Yaramasu, B. Wu, L. Tarisciotti, P. Zanchetta, and P. Wheeler, "Modulated model predictive control (m2pc) with fixed switching frequency for an npc converter," in *process IEEE 5th International Conference on Power Engineering, Energy and Electrical Drives (POWERENG)*, May 2015, pp. 623–628.
- [13] M. Rivera, M. Pérez, C. Baier, J. Muñoz, V. Yaramasu, B. Wu, L. Tarisciotti, P. Zanchetta, and P. Wheeler, "Predictive current control with fixed switching frequency for an npc converter," in *process 2015 IEEE 24th Int. Symp. Ind. Electron.*, June 2015, pp. 1034–1039.
- [14] F. Donoso, A. Mora, R. Cárdenas, A. Angulo, D. Sáez, and M. Rivera, "Finite-set model-predictive control strategies for a 3l-npc inverter operating with fixed switching frequency," *IEEE Trans. Ind. Electron.*, vol. 65, no. 5, pp. 3954–3965, May 2018.
- [15] J. Lee, J. Lee, H. Moon, and K. Lee, "An improved finite-set model predictive control based on discrete space vector modulation methods for grid-connected three-level voltage source inverter," *IEEE J. Emerg. Sel. Topics Power Electron.*, vol. 6, no. 4, pp. 1744–1760, Dec 2018.
- [16] L. Tarisciotti, P. Zanchetta, A. Watson, J. C. Clare, M. Degano, and S. Bifaretti, "Modulated model predictive control for a three-phase active rectifier," *IEEE Trans. Ind. Appl.*, vol. 51, no. 2, pp. 1610–1620, March 2015.